of accommodating Mo, V (or Fe). Feature c is compatible with ENDOR results[19] obtained for the Fe/Mo/S center in nitrogenase, and feature d is significant in view of the recent recognition of active nitrogenases where Mo is replaced by either vanadium (in an apparently similar Fe/V/S core structure[20]) or even iron.[21]

Acknowledgment. The support of this work by Grant GM-26671 from the National Institutes of Health is gratefully acknowledged. D.C. acknowledges useful discussions with Prof. W. H. Orme-Johnson.

Supplementary Material Available: A discussion presenting crystal and structural data for I, III, and IV and Tables S1-1–4 and S2-1–4, listing positional and thermal parameters and bond distances and angles for the Et_4N^+ salts of II and III (18 pages); Tables S1-5 and S2-5, listing structure factors for the Et_4N^+ salts of II and III (19 pages). Ordering information is given on any current masthead page.

(19) Hoffman, B. M.; Venters, R. A.; Roberts, J. E.; Nelson, M.; Orme-Johnson, W. H. *J. Am. Chem. Soc.* **1982**, *104*, 4711.
(20) (a) Eady, R.; Robson, R.; Postgate, J. *New Sci.* **1987**, *18*, 59. (b) Hales, B. J.; Case, E. E.; Morningstar, J. E.; Djeda, M. F.; Mauterer, L. A. *Biochemistry* **1987**, *25*, 7251. (c) George, G. N.; Coyle, C. L.; Hales, B. J.; Cramer, S. P. *J. Am. Chem. Soc.* **1988**, *110*, 4057.
(21) Hales, B. J. Personal communication.

Department of Chemistry
The University of Michigan
Ann Arbor, Michigan 48109

D. Coucouvanis*
P. R. Challen
Sang-Man Koo
W. M. Davis
W. Butler
W. R. Dunham

Received May 15, 1989

A Novel Ferromagnetic Inorganic–Organic Host–Guest System. Synthesis of Crystalline Small Magnetite Particles Complexed with Bis(pyridoxylidenehydrazino)phthalazine (DPDHP) at Ambient Temperature and Neutral pH

The naturally occurring "magnetic stone"—magnetite (Fe_3O_4)—was produced on earth some thousands of millions of years ago. Synthetically it is produced by the high-temperature oxidation of iron[1] or from mixed iron salts (Fe(II) and Fe(III)) in water and OH^- (pH > 13).[2] Polymer-anchored magnetite is produced from iron salts in water, O_2, OH^-, and polymeric lignosulfonate at elevated temperatures (90–140 °C) and pH (>12).[3] Magnetic bacteria and other biological systems, in contrast, can produce small magnetite particles at ambient temperature and pressure and neutral pH with defined crystallochemical characteristics by an unknown process.[4]

We wish to report the formation and characterization of novel types of host–guest molecules of general structures **3** and **4**, containing in crystalline forms small particles of magnetite sequestered by the title compound DPDHP[5] (L_A, **1**), by allowing ferrous sulfate to react with **1** at ambient temperature and pressure and neutral pH. The organic component (**1** and/or **2**) contains three azine (N–N) groups linked to two pyridoxylidene residues, thus forming a compartmental open-chain macrocycle with N_4O_2 sites for metal coordination[7,8] (see Schemes I and II).

Aqueous solutions of DPDHP hydrochloride[9] (**1**; 0.61 g, 1 mmol, in 150 mL of H_2O) and $FeSO_4 \cdot 7H_2O$ (1.12 g, 4 mmol, in 50 mL of H_2O) were first neutralized (pH 6.0)[13] separately by

Scheme I

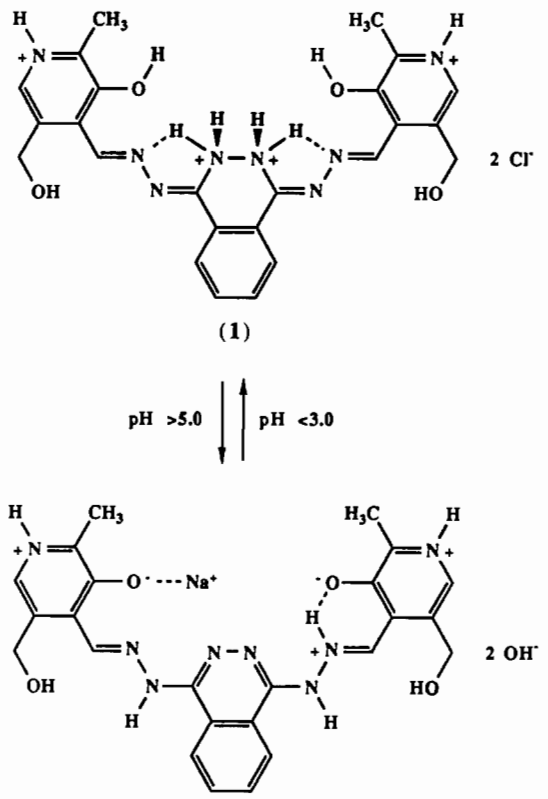

(1) Brett, M. E.; Graham, M. J. *J. Magn. Magn. Mater.* **1986**, *60*, 175.
(2) (a) Elmore, W. C. *Phys. Rev.* **1938**, *54*, 309. (b) David, I.; Welch, J. E. *Trans. Faraday Soc.* **1958**, *52*, 1642. (c) McNab, I. K.; Fox, B. A.; Boyle, Y. F. *J. Appl. Phys.* **1968**, *39*, 5703. (d) Brett, M. E.; Graham, M. J. *J. Magn. Magn. Mater.* **1986**, *60*, 171.
(3) Hassett, K. L.; Stecher, L. C.; Hendrickson, D. N. *Inorg. Chem.* **1980**, *19*, 416.
(4) (a) Review: Blakemore, R. P. *Annu. Rev. Microbiol.* **1982**, *36*, 217. (b) Mann, S.; Frankel, R. B.; Blakemore, R. P. *Nature (London)* **1984**, *310*, 405. (c) Paoletti, L. C.; Blakemore, R. P. *J. Bacteriol.* **1986**, *167*, 73.
(5) DPDHP was shown[6] to inhibit pyridoxal-dependent enzymes such as (i) glutamic acid decarboxylase, which generates γ-aminobutyric acid (GABA), (ii) DOPA decarboxylase, and (iii) glutamate-pyruvate transaminase.
(6) (a) Ackermann, E.; Oehme, P.; Rex, H.; Lange, P. *Acta Biol. Med. Ger.* **1964**, *12*, 322. (b) Oehme, P.; Rex, H.; Ackermann, E. *Acta Biol. Med. Ger.* **1964**, *12*, 284. (c) Oehme, P.; Niedrich, H.; Jung, F.; Rudel, M. *Acta Biol. Med. Ger.* **1969**, *22*, 345, 359.
(7) The tetraaza analogue dipyridoxylidene-*o*-phthaldehyde dihydrazone (L_B), appearing in **4**, **5**, **6**, and **8**, is assumed to act as a tetradentate sequestrant.
(8) Compare: (a) Andrew, J. E.; Blake, A. B. *J. Chem. Soc. A* **1969**, 1412. (b) Ball, P. W.; Blake, J. E. *J. Chem. Soc. A* **1969**, 1415.
(9) Commerical pyridoxal hydrochloride (0.4 g, 2 mmol) and dihydrazinophthalazine hydrochloride (0.26 g, 1 mmol) were dissolved respectively in 10 and 30 mL of 1:1 H_2O–MeOH and then mixed and stirred for 3 h at room temperature. MeOH (30 mL) was added and a red-orange precipitate (0.66 g) of DPDHP collected. Recrystallization from EtOH afforded red crystals, mp 250 °C. Anal. Calcd for $C_{24}H_{24}N_8O_4 \cdot 3HCl \cdot 2H_2O$: C, 45.48; H, 4.89; N, 17.67. Found: C, 45.73; H, 4.67; N, 17.64. When it is heated in vacuo (140 °C), it loses $^1/_2$ HCl without a noticeable change in color but its melting point increases to 275 °C. Anal. Calcd for $C_{24}H_{24}N_8O_4 \cdot 2H_2O$: C, 46.81; H, 4.96; N, 18.20; Cl, 14.42. Found: C, 46.67; H, 4.82; N, 17.46; Cl, 14.50. ^1H NMR (300 MHz, DMSO-d_6, 25 °C): δ 8.87 (s, 2 H, CH=N), 8.39, 8.01 (s, 2 H, pyridinic), 7.97, 7.96, 7.94, and 7.93 (4 H, aromatic), 4.69 (d, 4 H, CH_2O), 3.60–3.34 (m, 6 H, OH and NH), 2.52, 2.51, and 2.49 (s, 6 H, CH_3). UV (EtOH): λ_{max} 417, 391, 385, 305, 274, and 218 nm.[10,11]
(10) UV (EtOH) λ_{max} bands at 390 and 280 nm, for the unprotonated free base of DPDHP (L_A), are reported in: Oehme, P. In *Pyridoxal Catalysis: Enzymes and Model Systems*; Snell, E. E., Braunstein, A. E., Severin, E. S., Torchinsky, Yu. M., Eds.; New York, 1968; pp 677–692.
(11) The observed spectrum is assumed to be composed of three subspectra (λ_{max}): (i) 417, 385, 274 nm; (ii) 391, 274 nm; (iii) 305, 218 nm.[12]
(12) Compare: (a) Heinert, D.; Martell, A. E. *J. Am. Chem. Soc.* **1963**, *85*, 188. (b) Matsushima, Y.; Martell, A. E. *J. Am. Chem. Soc.* **1967**, *89*, 1322, 1331. Also: Sala, L. F.; Martell, A. E.; Motekaitis, R. J.; Abbott, E. H. *Inorg. Chim. Acta* **1987**, *135*, 123.

0020-1669/89/1328-4183$01.50/0

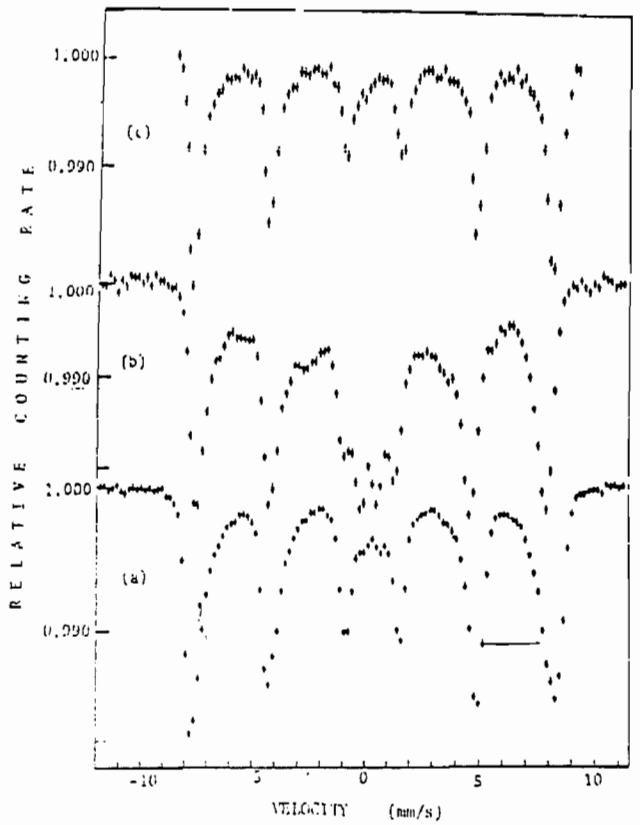

Figure 1. ^{57}Fe Mössbauer spectra obtained for (a) sample **6** at 90 K, (b) sample **6** at 300 K, and (c) sample **8** at 300 K.

adding 3 and 2.5 mL of 1 N NaOH, respectively, and then combined with stirring and the pH was adjusted to 7.0 ± 0.2 with dilute NaOH. The color of the resulting solution varied successively from shades of green to dark brown. No spontaneous precipitation was noted after standing overnight or on subsequent boiling for 10 min. Removal of water in vacuo left a black-brown solid residue (1.1 g), highly magnetic, which was dissolved in 2 L of methanol. To induce crystallization, 80% of the methanol was removed (reduced pressure) and diethyl ether carefully added. The black crystalline product (**5**) was cubic, containing 18% iron,[14] corresponding to a composition of $L_A[Fe_3O_4]_3L_B(SO_4)_{1.3}OH$, namely, a 1:4.5 ligand to Fe ratio[15] or a 1:0.77 pyridoxylidene residue to $[Fe_3O_4]$ ratio.

When the respective solutions of L_A (192 mg in 45 mL of H_2O) and $FeSO_4$ (336 mg in 45 mL of H_2O) were mixed at room temperature, an immediate yellow coloration was noticed, which changed gradually into dark green on adding dropwise 0.1 N NaOH until pH 7.0 was reached. Boiling the reaction mixture for 10 min yielded a magnetic black-brown precipitate (266 mg). It was washed with hot methanol, dried, and recrystallized from dimethyl sulfoxide (DMSO), to yield highly magnetic black microcrystals. It was analyzed as a host–guest compound containing 27.47% iron, corresponding to the composition $[Fe_3O_4]_{4.67}(C_{48}H_{44}N_{15}O_8)(SO_4)_{2.25}\cdot H_2O$[16] (**6**; see Chart I) namely, a

Chart I. Possible Structures of Small Particles of Organomagnetities (L:Fe = 1:7; Sample **6**)

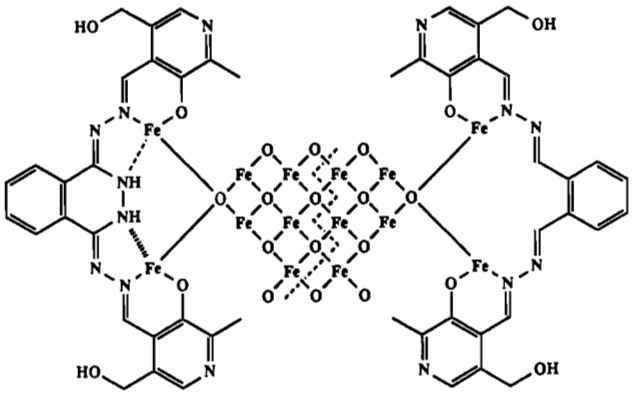

Coplaner

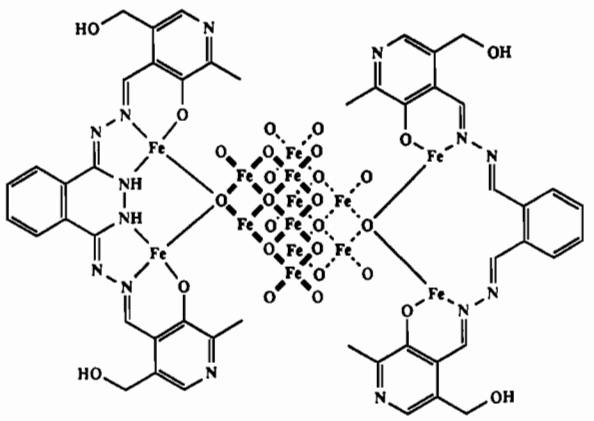

non-Coplaner

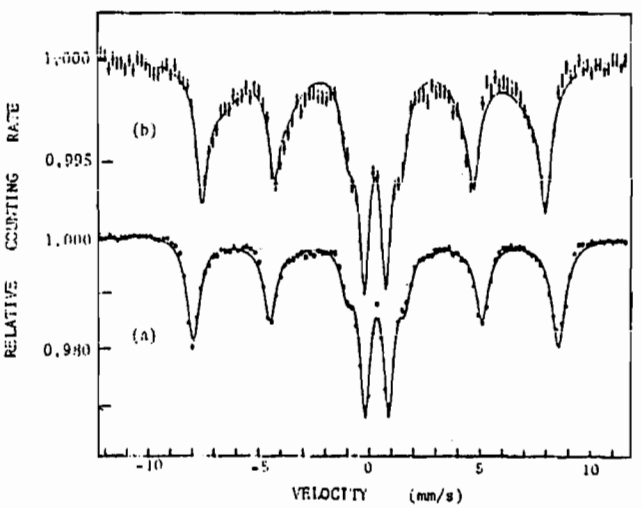

Figure 2. ^{57}Fe Mössbauer spectra obtained for sample **5** at (a) 90 K and (b) 300 K.

(13) At pH 6.0 the orange-red DPDHP hydrochloride turned yellow. It was analyzed as the $C_{24}H_{23}N_8O_4Na\cdot1.5H_2O$ compound, mp 230–232 °C. UV (EtOH): λ_{max} 412, 305 (sh), 276 (sh), 212 nm. IR (Nujol, cm^{-1}): 3360 m, 3170 w, 3020 w, 2710–2590 m, 1610 m, 1595 s, 1550 s, 1410 s, 1395 s, 1380 s, 1275 s, 1150 s, 1010 s, 1000 s, 960 m, 760 s, 700 s. ^{1}H NMR (300 MHz, DMSO-d_6): δ 8.89 (s, 2 H), 8.46 (s, 1 H), 8.42 (s, 1 H), 7.92, 7.90, 7.87, 7.85 (4 H, aromatic), 4.69 (s, 2 H), 4.49 (s, 2 H), 3.87, 3.23 (m, 4 H), 2.43, 2.40, 2.36 (s, 6 H). Anal. Calcd for $C_{24}H_{22}N_8O_4Na\cdot0.5H_2O$: C, 53.23; H, 4.25; N, 20.70. Found: C, 53.50; H, 5.07; N, 20.57.

(14) Anal. Found: C, 20.40; H, 1.49; N, 7.07; S, 1.40; Fe, 18.0.

(15) Ferromagnetic and/or paramagnetic products were obtained, depending on the pH and the iron salt:ligand ratio in the reacting system. Thus, at pH lower than 6.0 the preponderant product was composed of $L_AFe_2SO_4\cdot2H_2O$, a dark brown nonmagnetic powder. Anal. Calcd for $C_{24}H_{26}N_8O_{10}SFe_2$: Fe, 15.34. Found: Fe, 15.00. At pH ≥ 6.5, a 50:50 mixture of ferromagnetic and paramagnetic particles[17] (**3a**) was obtained. Anal. Calcd for $C_{24}H_{28}O_{16}SFe_{3.45}$: C, 31.68; H, 3.08; N, 12.32; Fe, 21.25. Found: C, 31.60; H, 2.84; N, 12.14; Fe, 21.20. This corresponds to the composition $[Fe_3O_4]_{1.15}L_ASO_4\cdot3H_2O$. If the iron salt:ligand ratio was increased to 4:1 (pH > 8.0), ferromagnetic particles (100%) were obtained, with the composition $[Fe_3O_4]_{2.67}L_A(SO_4)_2\cdot3H_2O$ (**3b**). Anal. Calcd for $C_{24}H_{26}N_8O_{26}S_2Fe_8$: Fe, 33.08. Found: Fe, 32.26. Under slightly different conditions (pH 7.2) other ferromagnetic particles (**4**) were obtained, of the composition $[Fe_3O_4]_{1.6}L_B(SO_4)_{1.25}\cdot3H_2O$. Anal. Calcd for $C_{24}H_{26}N_6O_{18.5}S_{1.25}Fe_{4.7}$: Fe, 26.4. Found: 26.3 (see Scheme III).

Scheme II

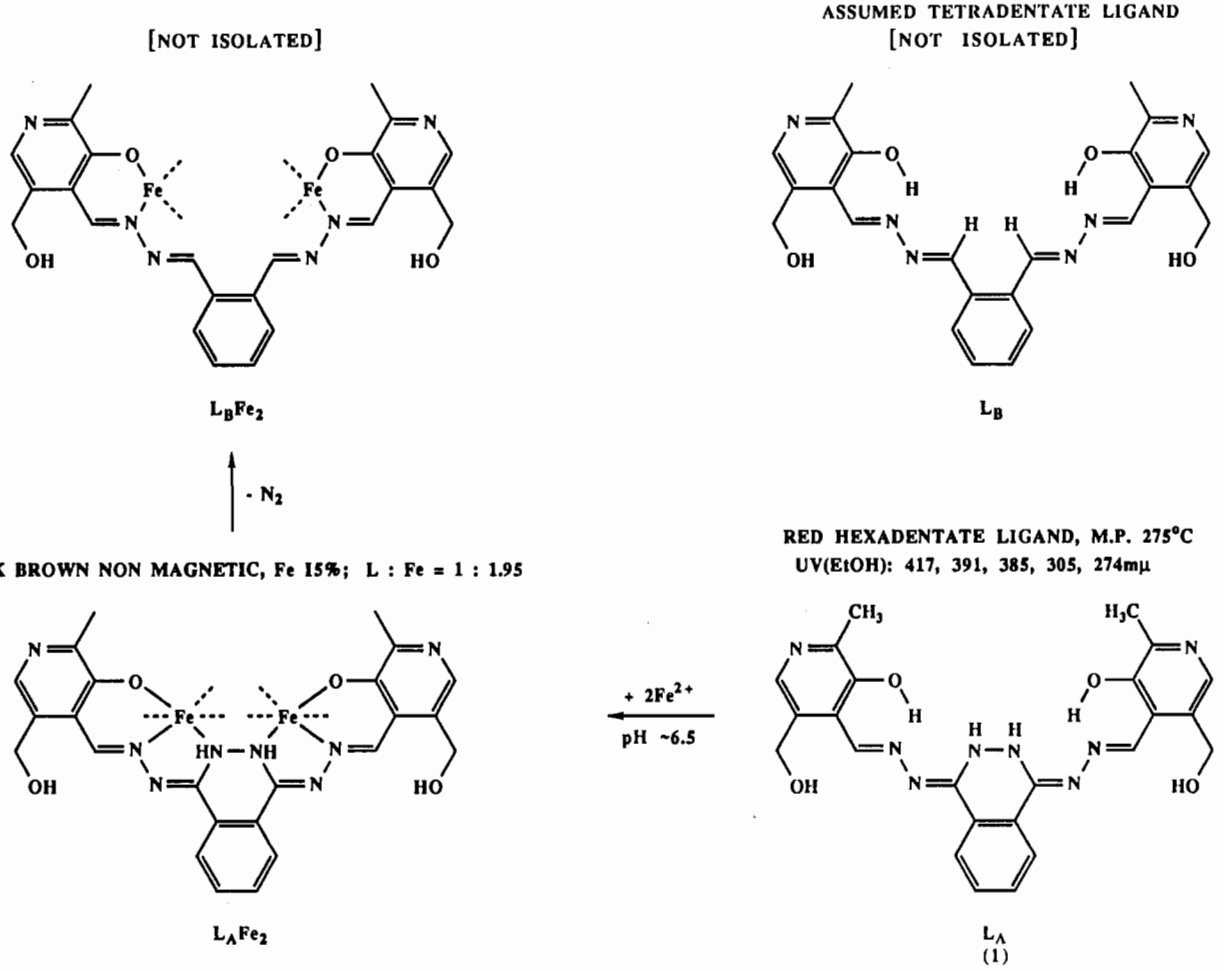

1:7 ligand to Fe ratio or a 1:1.17 pyridoxylidene residue to $[Fe_3O_4]$ ratio.

The presence of small particles of magnetite in sample **5** was deduced from (i) Mössbauer spectroscopic measurements, (ii) magnetization, (iii) X-ray powder diffraction, and (iv) electron diffraction.

Mössbauer spectroscopy measurements of all samples have been performed over a wide temperature range.[17] The corresponding Mössbauer spectra obtained for samples **6** and **5**, at 90 and 300 K, are shown in parts a and b of Figure 1 and in Figure 2, respectively.[18] The spectrum of **6** at 90 K is composed mainly of magnetic sextets with somewhat broadened absorption lines. The spectrum at 300 K shows much broader absorption lines and additional lines of low intensity in the central part of the spectrum. The Mössbauer parameters and the shape of the spectra at various temperatures are very characteristic of small particles of Fe_3O_4. A comparison of the spectra obtained here with those given by McNab et al.[2c] gives an average particle size diameter of 120 Å.

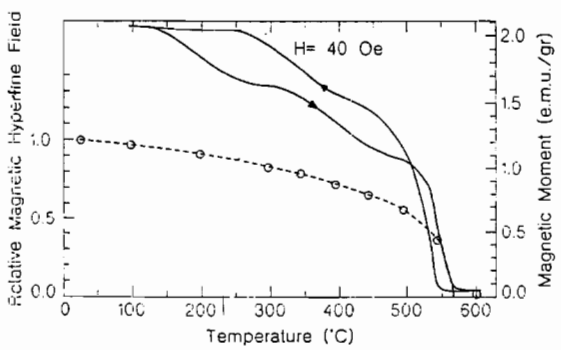

Figure 3. Specific magnetization obtained at an external field of 40 Oe for sample **5** (solid lines) and magnetic hyperfine field obtained from Mössbauer measurements on **5** as a function of temperature (dashed line). The arrows indicate the heating and cooling curves in the magnetization measurements.

The temperature dependence of the magnetic hyperfine splitting is given in Figure 3. From this curve the magnetic ordering temperature of 570 °C can be established. The Mössbauer spectrum of sample **8** obtained after heating sample **6** to 600 °C for several hours shows at 300 K well-defined absorption lines much narrower than those observed in sample **5** and no additional lines in the center (Figure 1c). Nevertheless this spectrum does not resemble Fe_3O_4 bulk spectra but rather those obtained for small Fe_3O_4 particles of an average diameter of 160 Å.[2c] It thus seems that heating sample **6** to 600 °C causes an aggregation process of the Fe_3O_4 particles, which increases their diameter.

The Mössbauer spectrum of sample **5** was composed of a superposition of three subspectra: magnetic sextets as observed in samples **6** and **8** and a quadrupole doublet that had at 90 K a splitting of 1.06 ± 0.02 mm/s and an isomer shift of 0.46 ± 0.01 mm/s relative to metallic iron. An example of such spectra is

(16) Anal. Found: C, 19.86; H, 1.64; N, 7.15; S, 2.50; Fe, 27.47.
(17) Mössbauer spectra were taken on a conventional Mössbauer constant-acceleration spectrometer with a 100-mCi ^{57}Co:Rh source. The hyperfine parameters were obtained by the procedure of a least-squares fit of theoretical spectra to those observed experimentally.
(18) Computer fits to these spectra (solid lines) show that the spectra are composed of a quadrupole doublet, with parameters given in the text, and two magnetic subspectra: At 90 K the hyperfine fields are 513 ± 3 and 480 ± 20 kOe and the isomer shifts relative to metallic iron at room temperature are 0.42 and 0.9 mm/s, respectively. The spectrum with the lower field is composed of appreciably broadened lines and covers about 30% of the magnetic area. The spectrum at 300 K is also composed of two magnetic subspectra: one has a field of 480 ± 3 kOe and isomer shift of 0.31 mm/s; the other, with broadened lines, has a magnetic field of 445 ± 5 kOe and an isomer shift of 0.45 mm/s and covers about 50% of the magnetic spectrum. These parameters are similar, yet not identical with, those found in bulk Fe_3O_4.[2c,d]

Scheme III

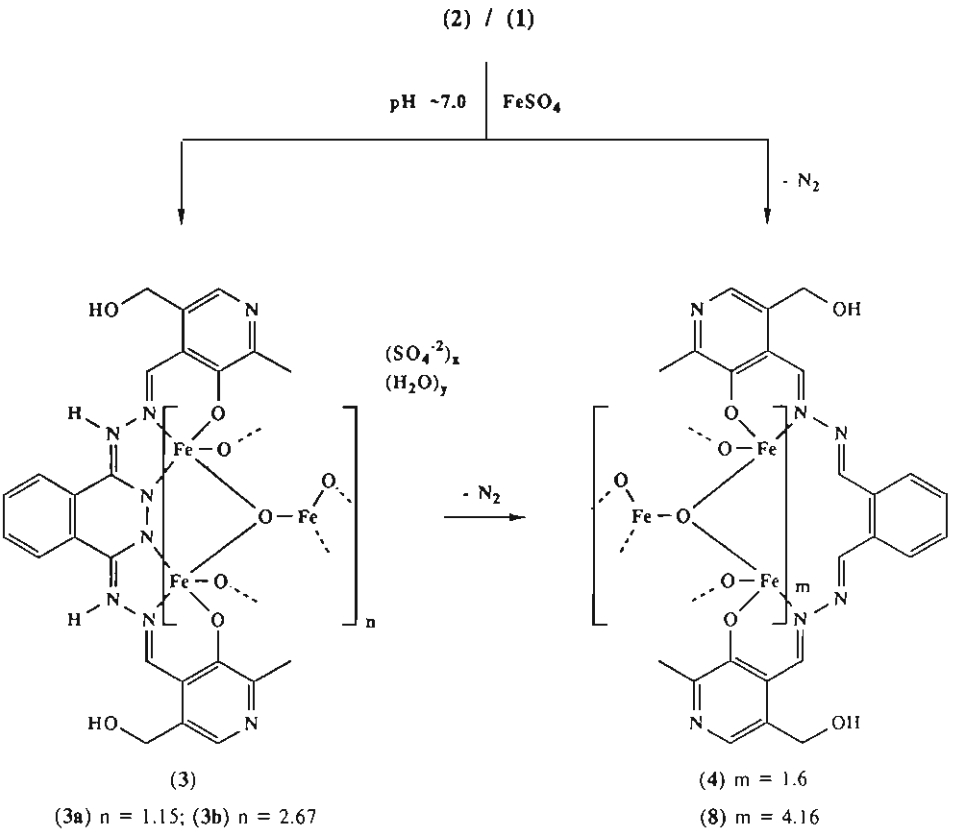

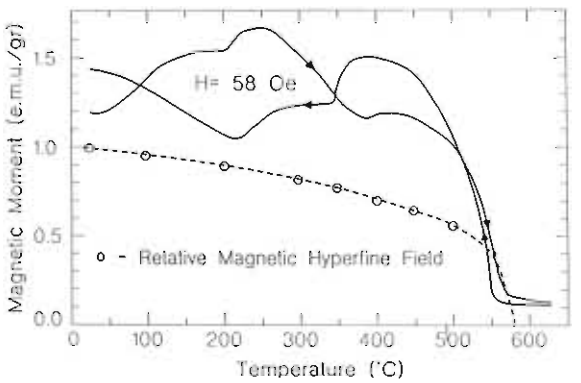

Figure 4. Solid lines: Specific magnetization obtained at an external field of 58 Oe for sample **6** (solid lines) and magnetic hyperfine field obtained from Mössbauer measurements on **6** as a function of temperature (dashed line). The arrows indicate the heating and cooling curves in the magnetization measurements.

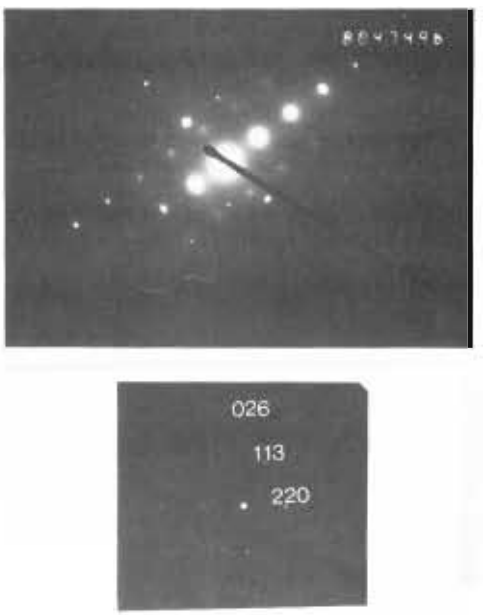

Figure 5. Electron diffraction pattern of sample **5** corresponding to the [110] zone.

shown in Figure 2.[18] The relative intensity of the doublet[19] decreases somewhat as the temperature is raised and therefore cannot be due to superparamagnetism of the Fe_3O_4 particles but rather to different iron sites in the sample. The decrease of the relative intensity of this doublet with increasing temperature indicates that the bonding of the iron in the sites responsible for this doublet is weaker than the bonding of the iron in the Fe_3O_4 sites.

The plots of the specific magnetization[20] σ_m against temperature of both **6** and **5** (heating curve) show, in good agreement with the Mössbauer measurements, the characteristic ordering temperature for Fe_3O_4 at 570 °C (Figures 3 and 4). The cooling curves (Figures 3 and 4), however, are notably different from the heating curves. This change is presumably due to the changes in particle size or fragmentation–coalescence processes[21,22] taking

(19) Ratios based on Mössbauer spectroscopic measurements.[17]

(20) Magnetic susceptibilities were measured on a PAR 155 VSM magnetometer. The samples were in a low magnetic field (40–60 Oe), and the temperature was raised at a rate of 5 °C/min.

(21) Sample **8** was obtained after heating **6** to 600 °C. Anal. Calcd for $C_{24}H_{24}N_6O_{20.6}S_{2.25}Fe_{12.5}$: C, 19.22; H, 1.60; N, 5.60; S, 4.80; Fe, 46.72. Found: C, 19.37; H, 1.63; N, 5.38; S, 4.68; Fe, 46.52. This corresponds to the composition $[Fe_3O_4]_{4.16}C_{24}H_{24}N_6O_4S_{2.25}$, namely, a 1:12.5 ligand:Fe ratio or a 1:2.08 ratio for pyridoxylidene:$[Fe_3O_4]$.

place while the sample is heated to 600 °C.

The X-ray diffraction pattern of **6** clearly displays all the peaks that characterize the Fe_3O_4 spinel structure.[23] Before it was heated, **5** appeared somewhat amorphous, displaying only hints of the peaks that were observed in the crystalline particles of **6**.

The crystals of **5** gave good single-crystal electron diffraction patterns[24] but were not stable in the electron beam. In this respect they are quite unlike Fe_3O_4 itself. Electron diffraction on the crushed material revealed several cleavage planes, in particular the [100] and [$\bar{1}$10] zones. The selected area diffraction pattern corresponding to the [$\bar{1}$10] zone is given in Figure 5. All patterns are entirely consistent with a fundamental Fe_3O_4 lattice, with in some cases powder rings arising due to decomposition of the material under the electron beam.

The organic molecules in the magnetic products described above are thought to be directly bonded to the inorganic material via the pyridoxylidene moieties. Chart I delineates possible structures for the small particles of **6** as well as for **5** after due adjustments. The pyridoxylidene:[Fe_3O_4] ratios vary from 1:0.77 in **5** to 1:1.17 in **6**, to 1:1.34 in **3b**, to 1:2 in **8**, and to 1:3 in **7**. When it is heated to 600 °C, a dimer of **6** loses formally one unit of L_AFe_2 to yield **8**, in which the stoichiometric ratio of 1:12 for ligand:Fe appears to be most favorable for the highest magnetic ordering. The alignment of the organic molecules within the inorganic lattice structure is currently under study.

(22) Sample **7** was obtained from sample **5** after heating to 570 °C. Its analysis corresponded to the composition $[Fe_3O_4]_3$(pyridoxylidene)·$1.5H_2O$, implying a loss of the labile dihydrazinophthalazine moiety from sample **5**. Anal. Calcd for $C_8H_{12}NO_{15.5}Fe_9$: C, 10.98; H, 1.37; N, 1.60. Found: C, 10.81; H, 1.29; N, 1.32.

(23) The *d* values and the relative intensities of peaks are as follows: 2.960 A [220], 30%; 2.529 Å [311], 100%; 2.094 Å [400], 20%; 1.610 Å [511], 30%; 1.482 [440], 40%. The pattern contains also some undefined peaks. The *a* lattice parameter was 8.376 Å.

(24) Single crystals of **5** were examined by using a JEOL JEM 2000FX electron microscope in the conventional manner. The largest crystals were ca. 1 μm in length.

Department of Pharmaceutical Chemistry
Hebrew University of Jerusalem
P.O. Box 12065
Jerusalem, Israel

Shalom Sarel*
Schelly Avramovic-Grisaru

Racah Institute of Physics
Hebrew University—Givat Ram
Jerusalem, Israel

E. Rivka Bauminger
Israel Felner
Israel Nowik

Inorganic Chemistry Laboratory
University of Oxford
South Parks Road
Oxford, U.K.

R. J. P. Williams
Nigel P. Hughes

Received April 25, 1989

Ground- and Excited-State Properties of a Photostable Hemicage Ruthenium(II) Polypyridine Complex

The properties of the long-lived, luminescent, metal-to-ligand charge-transfer (MLCT) state characteristic of (polypyridine)-ruthenium(II) complexes enable these compounds to sensitize photoinduced electron-transfer and energy-transfer processes. One limitation to the usefulness of these complexes as photosensitizers arises from the existence of a metal-centered (d–d) excited state that can be thermally populated from the ^{3}MLCT state. In addition to compromising the excited-state lifetime by providing an additional pathway for decay of the ^{3}MLCT state, crossover to the d–d state limits the photostability of the complex. Ligand dissociation from the distorted d–d state occurs with significant quantum yields, particularly in solvents of low dielectric constant and in the presence of coordinating ions (Cl^-, Br^-, NCS^-).[1,2]

Recent efforts to design $Ru(bpy)_3^{2+}$ type complexes (bpy is 2,2′-bipyridine) that are stable toward ligand photosubstitution have utilized three approaches: (1) synthesis of mixed-ligand complexes of the type $Ru(bpy)_2L_2$, where L is a nonchromophoric ligand with stronger σ-donor or π-acceptor properties, thus increasing the energy of the d–d state,[3] (2) synthesis of mixed-chelate $Ru(bpy)_2L$ complexes, where L is a modified chromophoric ligand with a lower lying π* level, thus decreasing the ^{3}MLCT energy,[4] and (3) synthesis of cage-type polypyridine complexes in which the three bipyridine ligands are covalently linked and provide an octahedral coordination environment in which the metal is encapsulated.[5,6a] The first two of these approaches involve increasing the energy barrier between the ^{3}MLCT and d–d states, whereas the third approach involves prevention of ligand dissociation. In addition, caging is expected to change the shape of the excited-state potential energy wells, especially for large nuclear displacements. Therefore, changes in the rates of radiationless decay processes, particularly those involving extensive nuclear distortions, are expected as a consequence of caging.[7]

As a step toward the design of this class of cage complexes, a series of bipyridine and phenanthroline macrobicyclic ligands has been reported.[8] Ruthenium complexes of these have not been prepared, however, possibly due to the insufficient size of the "cavity" provided. Recently a closed-cage amide-linked tris(bipyridine) complex, prepared with use of the Ru(II) ion as a template, was reported.[6b] When compared to $Ru(bpy)_3^{2+}$, this cage complex exhibited an increased excited-state lifetime at room temperature, as well as a dramatically decreased quantum yield for photosubstitution.[6a]

We report here the preparation of a novel ligand, $(Mebpy)_3Bz$, consisting of three 5,5′-dimethyl-2,2′-bipyridine (5,5′-dmb) groups linked to a central benzene ring via only methylene groups. The

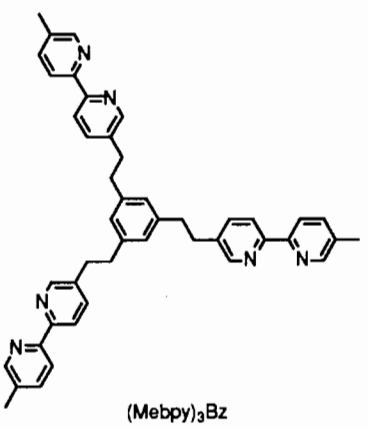

$(Mebpy)_3Bz$

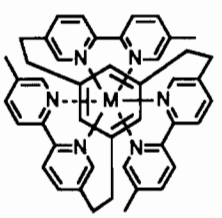

$[M((Mebpy)_3Bz)]^{n+}$

synthesis of $(Mebpy)_3Bz$ involves the reaction of the carbanion of 5,5′-dmb with 1,3,5-tris(bromomethyl)benzene in a 3:1 ratio.[9]

(1) Durham, B.; Caspar, J. V.; Nagle, J. K.; Meyer, T. J. *J. Am. Chem. Soc.* **1982**, *104*, 4803.
(2) Van Houten, J.; Watts, R. J. *Inorg. Chem.* **1978**, *17*, 3381.
(3) Caspar, J. V.; Meyer, T. J. *Inorg. Chem.* **1983**, *22*, 2444.
(4) Allen, G. H.; White, R. P.; Rillema, D. P.; Meyer, T. J. *J. Am. Chem. Soc.* **1984**, *106*, 2613.
(5) Balzani, V.; Juris, A.; Barigelletti, F.; Campagna, S.; Belser, P.; von Zelewsky, A. *Coord. Chem. Rev.* **1988**, *84*, 85.
(6) (a) DeCola, L.; Barigelleti, F.; Balzani, V.; Belser, P.; von Zelewsky, A.; Vogtle, F.; Ebmeyer, F.; Grammenudi, S. *J. Am. Chem. Soc.* **1988**, *110*, 7210. Barigelletti, F.; DeCola, L.; Balzani, V.; Belser, P.; von Zelewsky, A.; Vogtle, F.; Ebmeyer, F.; Grammenudi, S. *J. Am. Chem. Soc.* **1989**, *111*, 4662. (b) Belser, P.; DeCola, L.; von Zelewsky, A. *J. Chem. Soc., Chem. Commun.* **1988**, 1057.
(7) Balzani, V.; Sabbatini, N.; Scandola, F. *Chem. Rev.* **1986**, *86*, 319.
(8) Rodriguez-Ubis, J. C.; Alpha, B.; Plancherel, D.; Lehn, J. M. *Helv. Chim. Acta* **1984**, *67*, 2264.

0020-1669/89/1328-4187$01.50/0